INDUCTION MOTOR ROTOR CAGE FAULT DIAGNOSIS WITH STOCKWELL AND WAVELET TIME-FREQUENCY STATOR CURRENT ANALYSIS

Marius MEDIA[1], Bogdan VENESCU[2]

This article presents ways of identifying induction motor rotor cage fault using Stockwell case analysis and Wavelet transform of the stator start-up current. Faults are simulated by the mathematical model of the three-phase induction machine. That specific induction machine has 28 rotor cage bars. It is shown that time-frequency analysis (that highlights the time variation concerning a stator current) allows an accurate identification of broken bars. This identification is done with both the Wavelet and the Stockwell transform, in order to compare efficiency.

Keywords: Induction Motor Diagnosis, Wavelet and Stockwell signal transforms

1. Introduction

Three-phase cage induction motors are commonly used in industrial applications in a wide range of fields, due to their simple and robust structure and low manufacturing cost. The reliability of an induction motor is of paramount importance for commercial and industrial applications; also, it is used in the nuclear field and in the military industry. A very important fact that concerns the induction motors drive systems is the one related to the fast way in which every small defect is spotted right at the beginning. This helped prevent accidents that could have led to major consequences in terms of energy saving and safety.

Something that often happens with induction motors is that the rotor cage bars tend to break, as it can be seen in Fig. 1, where a diagram containing the frequency regarding possible defects from asynchronous machines is presented. Various strategies are used in the evaluation of work conditions and in the monitoring of induction motors.

[1] PhD, Faculty of Electrical Engineering, University POLITEHNICA of Bucharest, Romania, e-mail (mediamarius@yahoo.com).
[2] PhD(ABD), Faculty of Electronics, University of Pitesti, Romania, email (bogdan.venescu@yahoo.com).

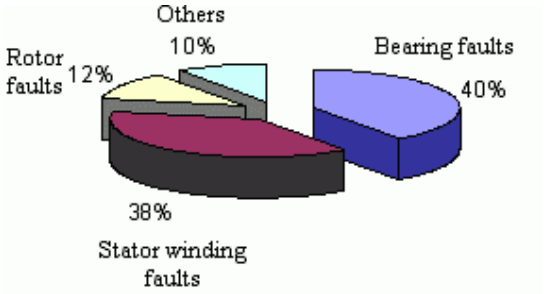

Fig. 1. Frequency of three-phase induction motor faults [1]

The motor's broken bars can be detected using methods which are recommended in different works (for instance, we can use the mechanical vibration analysis method [2], detection using air-gap torque spectra [3], spectral components study of angular speed signal [4]). The last method has a disadvantage [5]. Thus, the stator current becomes a parameter frequently used for asynchronous motor fault detection [6].

If the rotor bars break, they will produce a disturbance in the magnetic field of the machine's air gap, resulting in the appearance of some harmonics with certain frequencies in the machine's stator current. Frequencies of these harmonics depend on the "s" value of the machine and on the "f" frequency of her voltage power supply [7].

The current from the induction motor stator was used for fault diagnosis of the rotor bars in many works, works based on Park's vector analysis [8], or spectral analysis of stator current with Fourier transform [9]. Works in this specific field have presented different procedures in identifying the broken rotor bars and they all made use of the waveform analysis of the stator current. In [10] and [11], it is clear that we are dealing with broken bars, since a discrete wavelet transform (DWT) has been used to meassure (approximately and in detail) the levels of energy belonging to the stator current signal wavelet decomposition. In [12] and [13], signals of coefficients are analysed, signals that resulted from the start-up current decomposition with DWT, in the broken bar diagnosis.

The subject of this paper concerns the induction motor start-up current signal with DWT, which consist in a frequency band analysis of wavelet decomposition at D5 and A4 (meaning detailed and approximated) level. The fault frequencies corresponding to broken bars are located inside frequency bands in this decomposition level. Broken bar diagnosis is performed using the graphic representation of A4 and D5 coefficient signals and D5 detailed energy values.

Also, a study regarding how the current frequencies are absorbed is performed. In this study, the induction motor is observed during a transitory regime in which we use signal transform suggested by Stockwell [14] for the rotor cage fault diagnosis.

The number of broken rotor bars can be Fig.d out only by examining the fundamental frequency contour and the 40-60 Hz range, obtained after studying how Stockwell transform (ST) affects the motor . When using ST, the energy values obtained, corresponding to the entire motor current signal, were used as fault indicators. At the end, ST and Wavelet energy values of the stator current signal are compared, so that they can be used as diagnosis tools for broken bars.

2. The mathematical model for rotor cage fault simulation of a three-phase induction motor

Fig. 2 shows the equivalent circuit for one of the phases of the induction motor. In a study of the rotor cage's second broken bar, we will use a mathematical model of the induction motor where we will write the coordinates "*a b c*". The asymmetries produced by the broken bars will be taken into account while adding an additional resistance (besides the rotor resistance) to each of the rotor phases [15].

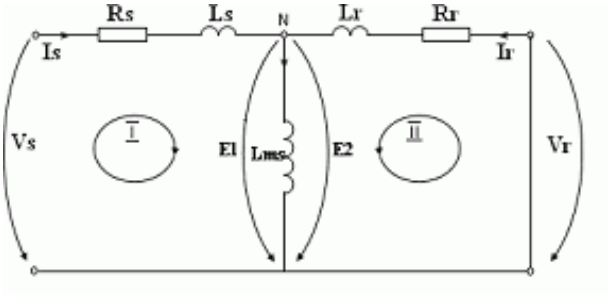

Fig. 2. The equivalent circuit for one of the phases of an induction motor

The basic induction motor equations in matrix form are the following (where a, b, c stand for phases & s, r stand for stator and rotor):

$$\text{Stator eq.:}\quad [V_{abc,s}] = [R_s]\cdot[i_{abc,s}] + [L_s]\cdot\frac{d}{dt}[i_{abc,s}] + [M_{sr}]\cdot\frac{d}{dt}[i_{abc,r}] \tag{1}$$

$$\text{Rotor eq:}\quad [V_{abc,r}] = [R_r]\cdot[i_{abc,r}] + [L_r]\cdot\frac{d}{dt}[i_{abc,r}] + [M_{sr}]^T\cdot\frac{d}{dt}[i_{abc,s}] \tag{2}$$

R_s, R_r are stator and rotor resistance matrices, and L_s, L_r, M_{sr} are stator, rotor, and mutual inductance matrices. The voltage, in each one of the three phases, is represented by $v_{as,}$ $v_{bs,}$ v_{cs} and the stator current by $i_{as,}$ $i_{bs,}$ $i_{cs.}$

$$[V_{abc,s}]=[v_{as}\ \ v_{bs}\ \ v_{cs}]^T$$
$$[i_{abc,s}]=[i_{as}\ \ i_{bs}\ \ i_{cs}]^T$$

$$[i_{abc,r}]=[i_{ar}\ \ i_{br}\ i_{cr}]^T \qquad (3)$$
$$[R_s]=R_s\text{diag}[1\ \ 1\ \ 1]$$
$$[R_r]=R_r\text{diag}[1\ \ 1\ \ 1]$$

The rotor resistance matrix in equation (3) will be modified for broken bar simulation and we get [16]:

$$[R_r]^* = \begin{bmatrix} R_{ra}+\Delta r_a & 0 & 0 \\ 0 & R_{rb}+\Delta r_b & 0 \\ 0 & 0 & R_{rc}+\Delta r_c \end{bmatrix} \qquad (4)$$

$$\text{Where: } \Delta r_{a,b,c} = \frac{3n_{br}}{N_b - 3n_{br}} R_r \qquad (5)$$

Δr_a, Δr_b and Δr_c represent variations in rotor resistance, variations regarding phase a, b and c, that have come to occur because of bar damage[17].
n_{br} and N_b represent the number of broken bars and the total number rotor bars. The function of rotor resistance changes $\Delta r_{a,b,c}$ because of the rotor faults.
The short-circuit rings and the magnetizing current aren't taken into account.

We made an experiment and we tested the methodology using a Matlab/Simulink model of the rotary three-phase induction motor at 1hp, 50 Hz, 4 poles and 200V [18]. The stator current waveforms that resulted from the Matlab/Simulink model of rotary three-phase induction motor, were confronted with other results [19].

Table 1

Parameters of the induction motor

Parameters	Value
Stator Resistance Rs	3.35 Ω
Rotor Resistance Rr	1.99 Ω
Stator Inductance Ls	6.94 mH
Rotor Inductance Lr	6.94 mH
Mutual Inductance Lm	163.73 mH
Rotor Bars Nb	28 bars
Rotor Inertia	0.1 kgm^2

3. Wavelet Transform

Wavelet Transform (WT) was developed as an alternative to short-time Fourier transform. WT calculates the dot product of the analyzed signal and a

wavelet family and provides simultaneous information regarding frequency and time.

The wavelet transform equation:

$$C(a,b)=\frac{1}{\sqrt{a}}\int_{-\infty}^{\infty}x(t)\Psi\left(\frac{t-b}{a}\right)dt \tag{6}$$

x(t) is the signal, a and b show the wavelet scale and position, Ψ(t) is the wavelet. A high scale corresponds to a low frequency stretched wavelet and a low scale wavelet corresponds to a high frequency compressed wavelet.

In the discrete wavelet transform case (DWT), filters having different cutoff frequencies are used to analyze the signal at different scales. The signal is passed through a series of high pass filters so that the high frequencies can be analyzed. After, it is passed through a series of low pass filters in order to analyze the low frequencies. The high pass filter coefficients are marked with D (from detail coefficients) and the low pass filter coefficients are marked with A from (approximate coefficients). The low frequency band extends from zero to half the Nyquist frequency where Nyquist frequency is $N=f_s/2$ (f_s-sampling frequency). After decomposing the signal, one can reconstruct and examine in detail the constituent components of the original signal.

In order to obtain fault components of motor current signal (around 50 Hz) with 6-level analysis lifting DWT, we used „*wavedec"* function from Matlab toolbox. The Db10 wavelet type from the Daubechies family was selected. Table 2 presents the frequency bands corresponding to the six levels of an A-phase motor current signal wavelet decomposition. A Db10 wavelet is used. The signal belonging to the D5 level in the wavelet decomposition, the one that has db10, can be used for rotor cage induction motors' fault detection, because their frequency band is between 32 and 64 Hz [20].

The sampling frequency for data acquisition is 1 kHz, and, from what we observed, the signal duration is 100 ms.

The total number of decomposition levels belonging to DWT signals, can be calculated with:

$$L=\frac{log(fs/f)}{log(2)}+1 \tag{7}$$

Where: fs=sampling frequency, and f= signal frequency

Table 2.

Frequency bands for levels 6 of wavelet decomposition

Approximations "a_i"	Frequency Bands (Hz)	Details "d_i"	Frequency Bands (Hz)
a_6	[0-16,125]	d_6	[16,125-32,25]
a_5	[0-32,25]	d_5	[32,25-64,5]
a_4	[0-64,5]	d_4	[64,5-125]
a_3	[0-125]	d_3	[125-250]
a_2	[0-250]	d_2	[250-500]
a_1	[0-500]	d_1	[500-1000]

In Fig. 3, A4 and D5 coefficient signals of a I_A stator current with a one-dimensional signal wavelet decomposition was reconstructed using *"wrcoef"* function from MATLAB toolbox.

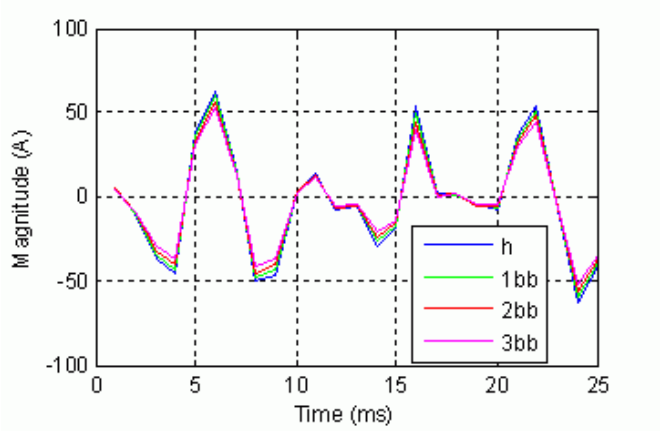

a) Signal of D5 detail level

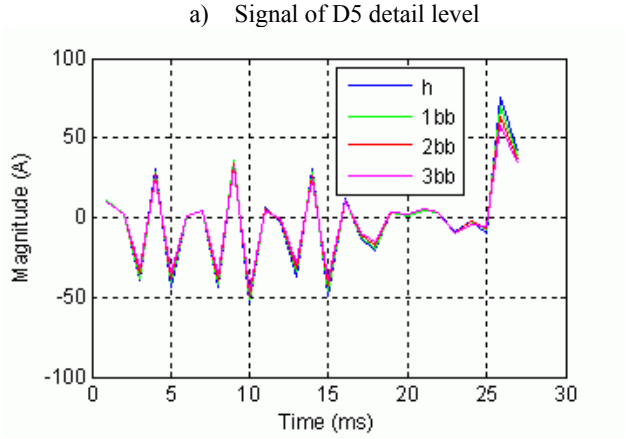

b) A4 approximation level

Fig.3. Wavelet decomposition levels of stator current signal (h-healthy, bb-broken bar)

2. Stockwell Transform

Inspired from the Wavelet and the Gabor transform, the Stockwell transform was presented to the public in 1996, its publishers being Stockwell, Mansinha and Lowe. ST can be derived from the WT by modifying the phase of the window function or mother wavelet. ST is an extension of WT. The phase of *S* transform provides time origin and gives us useful information about spectra that is not available in CWT.

In the case of a time-dependent signal *h(t),* ST can be seen as a product of the signal and a phase correction function $e^{(-j2\pi f\tau)}$.

The S-transform of *h(t)* is defined as:

$$S(\tau, f) = \int_{-\infty}^{\infty} h(t)\, g(\tau - t, f) e^{-i2\pi f t} dt \tag{8}$$

Where Gaussian window is: $g(t, f) = \frac{1}{\sigma\sqrt{2\pi}} \cdot e^{-\frac{t^2}{\sigma^2}}$ (9)

With $\sigma(f) = \frac{k}{|f|}$

Typical values of “k” are located between 0.2 and 3, allowing different frequency resolutions. High frequencies require a high value of "k" and low frequencies require a small one. Therefore, we obtain:

$$S(\tau, f) = \int_{-\infty}^{\infty} h(t) \frac{|f|}{k\sqrt{2\pi}} e^{-\frac{(\tau - t)^2 f^2}{2k^2}} e^{-i2\pi f t} dt \tag{10}$$

Where f is the frequency and t/τ is the time.

After this, we could resume the Wavelet transform as:

$$CWT(a, \tau) = \int_{-\infty}^{\infty} h(t) \psi(t - \tau, a) dt \tag{11}$$

S-transform can be defined as:

The multi-resolution ST is a complex matrix whose values from rows and columns are values regarding frequency and time. Each column shows the local spectrum in terms of time [21], [22].

Fig.5 shows the ST frequency spectrum of the I_A stator transient current, for a healthy motor, in the absence of a load.

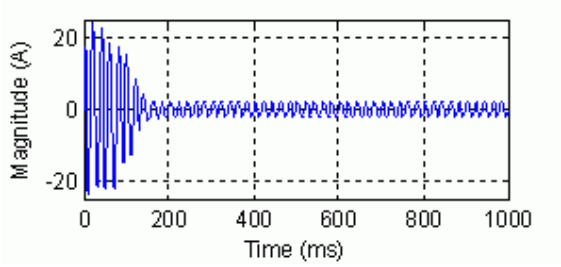

Fig.4. Stator current signal in A phase

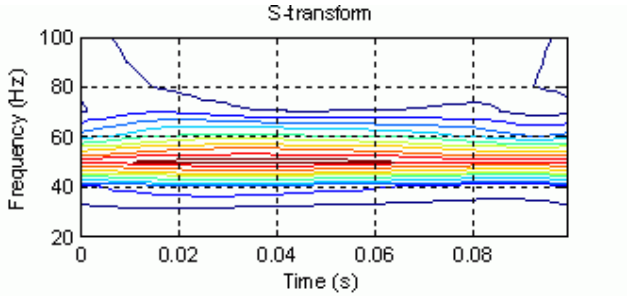

Fig.5 S-transform Time-Frequency contour

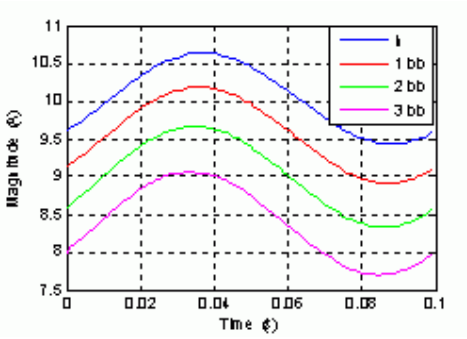

a) The fundamental frequency of ST contour

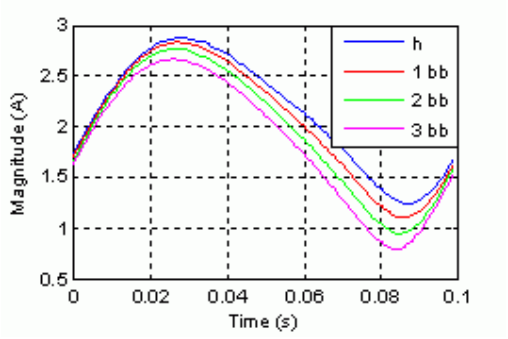

b) 40 Hz ST contour

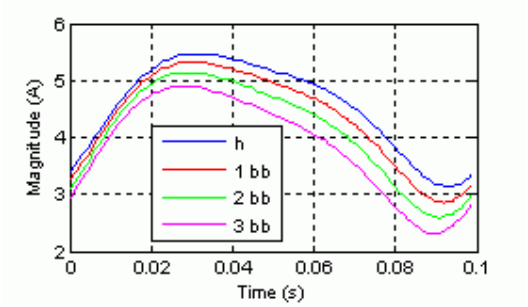

c) 60 Hz ST contour

Fig. 6. S-transform Time-Frequency contours (h-healthy motor, bb-broken bars)

Fig. 6 presents 40Hz, 50Hz and 60 Hz ST frequency contours of "I_A" stator current corresponding to different fault depths of the rotor's electrical circuit (this stands for a case in which the motor is in ztransient regime). The sampling frequency is 1 kHz, and the studied signal duration is 100 ms.

5. ST and WT energy of motor current signal

The start-up current signal of the induction motor is a non-stationary signal and its energy is calculated using Parseval's theorem. This can be mathematically expressed as [23]:

$$E_{DWT} = \sum_{n=1}^{N} |x(n)|^2 = \sum_{n=1}^{N} |a_j(n)|^2 + \sum_{j=1}^{m} \sum_{n=1}^{N} |d_j(n)|^2 \quad (13)$$

Where x(n) is discrete signal belonging to time domain, N is the total number of samples in the signal, $\sum_{n=1}^{N} |a_j(n)|^2$ is the total energy concentrated in level "j" of the approximated version of the signal, $\sum_{j=1}^{m} \sum_{n=1}^{N} |d_j(n)|^2$ is the total energy concentrated in a detailed version of the signal (from level 1 to m, where m is the maximum level of the wavelet decomposition).

We use DWT, in the case of a I_A stator current, as to obtain D5 wavelet decomposition coefficient signal energies for induction motor with 0, 1, 2 and 3 broken bars at various loads (Fig. 7).

Table.3.

Energy values of D5 detail coefficient of the A phase stator current signal

E_{D5}	Rotor faults			
	h	**1bb**	**2bb**	**3bb**
No load	29.89	30.26	30.61	30,88
Half load	29.24	29.30	29.49	29.82
Full load	29.98	29.92	29.92	30.07

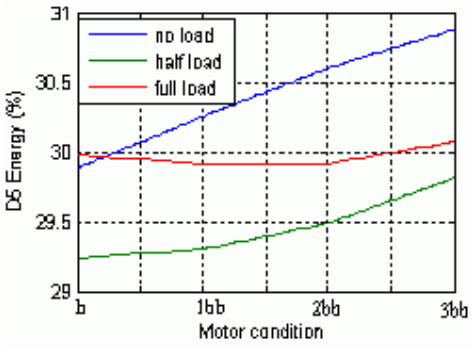

Fig.7.Energy of D5 wavelet decomposition level

In tables 4 and 5, the values for the signal energies required by ST are presented. Fig. 8 and 9 show graphics of energy values required by ST for the fundamental and total signal of the start-up current at various motor loads (in the case of different rotor cage fault).

Table 4

ST energy values for I_A current

E_{STfund}	**Rotor faults**			
	h	**1bb**	**2bb**	**3bb**
no load	1005.6	956.2	900.5	838.4
load 50%	1053.5	1006	951.2	888.9
Full load	1094.4	1049.6	996.7	934.8

Table 5

ST energy values for the total signal of I_A startup current

$E_{STtotal}$	**Rotor faults**			
	h	**1bb**	**2bb**	**3bb**
no load	137	129.7	122.7	116
load 50%	148.3	141.9	134.3	125.7
Full load	147.4	142.6	136.3	128.3

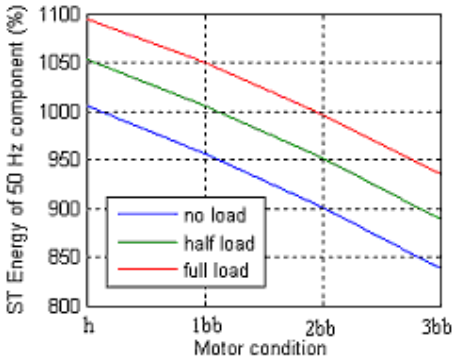

Fig.8. ST Energy of A phase current fundamental component

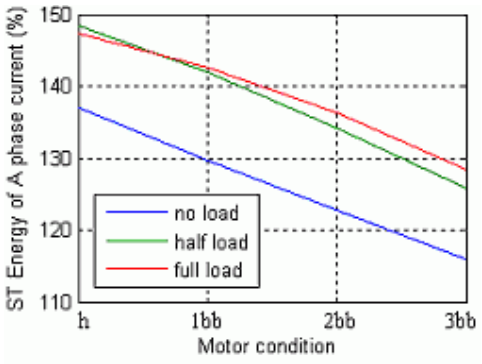

Fig. 9. ST Energy of A phase current

The report between the energy values of the D5 coefficient in the A phase starting motor current signal wavelet decomposition. We use Daubechies 10 (E_{D5}) corresponding to the healthy motor and the one that has faults (with 1,2 or 3 broken bars) and the same report for the fundamental component (E_{STfund}) and total signal (ESTtot) ST energies of I_A stator current presented in Table 7

$R= E_{D5h}/ E_{D51bb,\ 2bb,\ 3bb}$ (no load)

The "R" report can be considered an indicator of rotor fault.

Table 6

Table 7

Values of E_{D5}, E_{STfund}, E_{STtot}

No load	Rotor faults			
	h	**1bb**	**2bb**	**3bb**
E_{D5}	29.89	30.26	30.61	30,88
E_{STfund}	1005.6	956.2	900.5	838.4
E_{STtot}	137	129.7	122.7	116

Values of Report (R)

No load	Rotor faults		
	h/1bb	**h/2bb**	**h/3bb**
E_{D5}	0,987	0,976	0,967
E_{STfund}	1.05	1.11	1.19
E_{STtot}	1.06	1.12	1.18

Fig. 10 shows "R" values obtained with WT and ST for 1, 2 and 3 broken bars, when we have no load.

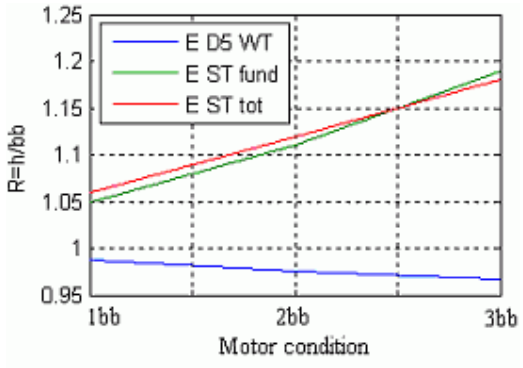

Fig.10. Fault indicator R= $E_h/E_{1bb,2bb,3bb}$

6. Conclusions

The main contribution consists in the fact that it provides a comparison between a technique of detecting the induction motor cage faults by extracting parameters of DWT coefficients of motor current reconstructed signal at different level, corresponding to different spectral bands and a cage fault detection technique using motor current ST analysis. The stator current waveform experimental data of the induction motor with cage faults will be analyzed.

An on-line diagnosis of the rotary three-phase induction motor's broken bars, containing the characteristics of the A4 approximation and D5 detail signals of DWT analysis (similar to Fig. 3), becomes necessary in revealing incipient faults of the induction motor rotor cage.

Fig. 6 shows graphics of the fundamental frequency contour of the stator current at 40Hz and 60Hz ST. We can observe the difference between several rotor fault depths and the number of broken rotor bars.

Also, in Table 6, the faults are highlighted through the ST energy values of the entire signal and fundamental component of the transient current and by the energy values of D5 wavelet decomposition level.

The ST energy value of the fundamental component is greater than DWT energy value of D5 decomposition level for 1, 2 and 3 broken bars.

In Fig. 10, the "R" fault indicators for ST energy have a higher value than 1 and a directly proportional evolution with the depth of fault. DWT energy of D5 signal has a value smaller than 1 and an inversely proportional evolution.

Acknowledgment

This work was supported by the Operational Program of Human Resources Development, 2007-2013, of the Romanian Ministry of Labor, Family and Social Protection, through the Financial Agreement POSDRU/88/1.5/S/ 61178.

R E F E R E N C E S

[1] *Ramin Salehi Arashloo, Alireza Jalilian*, "Induction Motor Broken Rotor Bar Fault Detection Using Discrete Wavelet Transform", 24th International Power System Conference 2009.

[2] D. *Mori., T. Ishikawa.,* "Force and vibration analysis of induction motors", IEEE Transaction on Magnetics, vol. 41, no. 5, May 2005, pp. 1948-1951.

[3] *Vinod V. Thomas, Member, IEEE, Krishna Vasudevan, and V. Jagadeesh Kumar, Member, IEEE*, "Online Cage Rotor Fault Detection Using Air-Gap Torque Spectra", IEEE Transactions on Energy Conversion, Vol. 18, No. 2, June 2003, pp. 265-270.

[4] *M. Media, F. Martin, Aurelian Crăciunescu and A. Rodriguez,* "Induction motor's broken bars detection by using Stockwell transform", International Symposium on Power Electronics, Electrical Drives, Automation and Motion-SPEEDAM, 21st Edition , Sorrento-Italy, June 20-22, 2012.

[5] *J.F. Watson, N.C.Paterson*, "Improved Techniques for rotor fault detection in three phase Induction Motors", 0-7803-4943-1998, IEEE, 1998.

[6] *A. Bellini, F. Filippetti, G. Franceschini, C. Tassoni, R. Passaglia, M. Saottini, G. Tontini, M. Giovannini, and A. Rosssi*, "Enel's experience with on-line diagnosis of large induction motors cage failures", IEEE Ind. App. Conf., vol.1, 2000, pp. 492-498.
[7] *M. Blodt, M. Chabert, J. Regnier, J. Faucher*, " Mechanical Load Fault Detection in Induction Motors by Stator Current Time-Frequency Analysis", IEEE Transaction on Industry Applications, vol. 42, n. 6, , 2006, pp.1454–1463.
[8] *M. Benouzza, M. Drif, A.J. Marques Cardos et J.A. Dente*, « Emploi de l'Approche des Vecteurs de Park pour la Détection des Défauts de Barres dans les Moteurs Asynchrones à Cage d'Ecureuil », Rev. Energ. Ren, 1999, pp. 71-76.
[9] *Abdelkader Mellakhi, Noureddine Benouzza, Azzedine Bendiabdellah,* « Analyse spectrale du courant statorique pour détecter les cassures de barres dans les moteurs asynchrones triphasés à cage en tenant compte des harmoniques d'espace », Revue Nature et Technologie, n° 02, Janvier 2010, pp. 35 - 40.
[10] *Jusso T. Olkkonen*, "Discrete Wavelet Transform-Theory and Applications", In Tech, ISBN 978-953-307-185-5, 2011, pag. 256.
[11] *S.K. Ahamed, S. Karmakar, M. Mitra, S. Sengupta*, "Diagnosis of Induction Motor Faults due to Broken Rotor Bar and Rotor Mass Unbalance through Discrete Wavelet Transform of Starting Current at No-Load", Journal of Electrical Systems, 6-3, 2010, pp. 442-456.
[12] *J. A. Antonino, M. Riera, J. Roger-Folch and V. Climente*, "Study of the startup transient for the diagnosis of broken bars in induction motors:A review", Departamento de Ingeniería Eléctrica E.T.S.I.I., Universidad Politécnica de Valencia, 2004.
[13] *N. Mehala, R. Dahiza,* "Rotor faults detection in induction motor by Wavelet analysis", International Journal of Engineering and Technology, Vol.1 (3) , 2009, pp.90-99.
[14] *R.G. Stockwell, L. Mansinha, R.P. Lowe,* "Localization of the complex Spectrum: the S-transform", IEEE Trans. on Signal Processing 44, 1996, pp.998-1001.
[15] *P. M. Santos, M. B. R. Correa, C. B. Jacobina, E. R. C. da Silva, A. M. N. Lima, G. Didiery, H. Raziky, and T. Lubiny*, "A simplified induction machine model to study rotor broken bar effects and for detection", PESC'06, 37th IEEE, Jun.2006, pp. 1-7.
[16] *Shuo Chen*, "Induction Machine Broken Rotor Bar Diagnostics Using Prony Analysis", Thesis for degree of Master of Engineering Science in Electrical Engineering, Adelaide, Australia, 2008.
[17] *F. Filippetti, M. Martelli, G. Franceschini and C. Tassoni*, "Development of expert system knowledge base to on-line diagnosisi of rotor electrical faults of induction motors", IEEE IAS Annu Meeting, Huston, Oct. 1992, pp. 92-99.
[18] *Chee-Mun Ong,* "Dynamic Simulation of Electric Machinery using Matlab/Simulink",
U.S.A. - Prentice Hall PTR –New Jersey, 1998, pp. 122-258.
[19] *Toshiji Kato, Kaoru Inoue, Daisuke Okuda,* "Diagnosis of multi-phase turn faults of induction motor stator windings", The International Conference on Power Electronics and Drive Systems-PEDS2009, pp. 144 -149.
[20] *Szabó, L., Dobai, J.B., and Bíró, K.Á.,* "Virtual Instruments for Detecting Rotor Faults in Induction Motors," Advances in Electrical and Electronic Engineering (Slovakia), no. 2, vol. 3, 2004, pp. 119-122.
[21] *Zbigniew Leonowicz, Tadeusz Lobos and Krzysztof Wozniak,* "Analysis of non-stationary electric signals using the S-transform", Eleventh IEEE Workshop on Control and Modeling for Power Electronics, COMPEL 2008, pp. 204-210.
[22] *Alejandro Rodríguez, Jose A. Aguado, Jose J. López, Francisco Martín, Francisco Muñoz and Jose E. Ruiz, Book*, "Time-Frequency Transforms for Classification of Power Quality Disturbances", Chapter Number 15, ISBN 978-953-307-180-0, April, 2011.

[23] *A. M. Gaouda, M.M.A. Salma, M.R. Sultan, A.Y. Chikhani,* "Power quality detection and clasification using wavelet decomposition", IEEE Transaction on Power Delivery, Vol.14, No.4, October 1999, pp. 1469-1476.